Science of Sintering, **54** (2022)401-414

https://doi.org/10.2298/SOS2204401Z

UDK: 546.824; 535.375; 621.926.087

Dielectric Properties of Mechanically Activated Strontium Titanate Ceramics

Jelena Živojinović[1*)], Darko Kosanović[1], Vladimir A. Blagojević[1], Vera P. Pavlović[2], Nenad Tadić[3], Branislav Vlahović[4,5], Vladimir B. Pavlović[6]

[1]Institute of Technical Sciences of the Serbian Academy of Sciences and Arts, Knez Mihailova 35/IV, 11000 Belgrade, Serbia

[2]University of Belgrade, Faculty of Mechanical Engineering, Kraljice Marije 16, 11120 Belgrade 35, Serbia

[3]University of Belgrade, Faculty of Physics, Studentski trg 12, 11000 Belgrade, Serbia

[4]North Carolina Central University, Durham, NC 27707, USA

[5]NASA University Research Center for Aerospace Device Research and Education and NSF Center of Research Excellence in Science and Technology Computational Center for Fundamental and Applied Science and Education, Durham, NC 27707, USA

[6]University of Belgrade, Faculty of Agriculture, Nemanjina 6, 11080 Belgrade, Serbia

Abstract:

In this study, microstructure evolution and dielectric properties of $SrTiO_3$ ceramic have been investigated, whereby mechanical activation of $SrTiO_3$ powders was used to modify the functional properties of ceramic materials. Microstructural SEM analysis of $SrTiO_3$ ceramics showed that the increase in mechanical activation time results in less porous samples. Raman spectroscopy indicated changes in the broadening and asymmetry of the TO_2 mode with a change in the time of mechanical activation. TO_2 mode showed a Fano asymmetry due to its interaction with polarization fluctuations in polar micro-regions, which are a consequence of the presence of oxygen vacancies caused by activation. The maximum value of dielectric permittivity was observed in the sample activated for 10 min. Also, the sample activated for 10 min exhibits relatively low values of loss tangent, compared to the other mechanically activated samples, providing the best overall dielectric performance compared to other samples.

Keywords*: XRD; SEM; Raman; Dielectric permittivity; $SrTiO_3$ ceramics.*

1. Introduction

Strontium titanate ($SrTiO_3$) is a quantum paraelectric material with cubic perovskite structure at room temperature [1,2]. $SrTiO_3$ has good insulating properties, making it suitable for the application in dynamic random access memories (DRAM) besides, it is also an efficient n-type semiconductor photocatalyst with a band gap of about 3.4 eV [3,4]. Due to its high dc-dielectric-field dependence on the dielectric constant it is suitable for tunable devices (tunable microwave phase shifters, filters, and resonators) [5] which are being developed to satisfy the constant development in microwave communication and data processing [6]. These

*) **Corresponding author:** jelena.zivojinovic@itn.sanu.ac.rs

require a dielectric material with relatively high tunability and low dielectric loss to achieve adjustment along with a wider range of the working frequencies, with low noise and high selectivity. $SrTiO_3$ has been recognized as a promising candidate material for these applications due to relatively low dielectric loss and high dielectric-field tunability [7].

The properties of a material are strongly affected by its microstructure and consequently by the method of synthesis. Precursor processing and sintering define the main characteristics of the materials, such as microstructure and the presence of defects, making the knowledge of the evolution of the microstructure during processing very important. Numerous methods, such as sol-gel [8], hydrothermal [9], combustion [10] and polymeric precursor [11] method, can be used for manufacturing $SrTiO_3$ materials. Most of these methods require high-purity chemicals, making them too expensive for industrial production. Therefore, commercial $SrTiO_3$ is still dominantly obtained by solid-state reaction [12]. The state-of-the-art application requires homogeneous micro-grain with low impurity levels of ceramic materials, making alternative low-cost effective methods for large-scale production of phase-pure and nanosized $SrTiO_3$ particles an important topic. The use of mechanical activation in high-energy mills can affect the evolution of the microstructure and sintering properties of the material [13]. Mechanical milling leads to a decrease in the particle size, which results in changes in dielectric properties of the ceramic material [14]. It has been established that a decrease in grain size to ~1 μm in some perovskites leads to an increase in the value of dielectric permittivity ($\varepsilon_r^{'}$), while a further decrease in grain size leads to a decrease in the value of $\varepsilon_r^{'}$ [15,16]. Also, the value of density of different activated sintered samples, i.e. different porosity, additionally affects the values of relative dielectric permittivity. A sample that has a high degree of porosity i.e. lower density, will have lower values of relative dielectric permittivity [17]. Generally, the microstructure has a major impact on the dielectric properties of $SrTiO_3$ ceramics and sintering is an important process that affects the evolution of the microstructure, grain growth, and densification [18,19]. During high-temperature sintering, it should be considered the formation of oxygen vacancies as a result of the loss of oxygen from the crystal lattice [20]. Oxygen vacancies may have an impact on the optical and electrical properties of $SrTiO_3$ and the ability to induce insulator-to-metal transition, as well as superconductivity [21-24]. The dielectric response, and other related properties of $SrTiO_3$, can be modified by controlling oxygen vacancy concentration and Sr/Ti ratio, through doping and substituting Sr and/or Ti ions [25-31]. In this regard, a precise control of defects to control the dielectric properties of perovskite-type oxides [32-35] is required, so establishing control over the concentration of oxygen vacancies is one of the most important issues in the development of multilayer capacitors [36, 37].

In this study, we will discuss the influence of mechanical activation of $SrTiO_3$ powders on the microstructure of sintered samples and the influence of relatively brief mechanical activation on dielectric properties in the activated $SrTiO_3$ perovskite-type oxide.

2. Materials and Experimental Procedures

As the starting material, a high purity commercial $SrTiO_3$ powder (99 % purity, mean particle size ≤ 5 μm) was used. The mechanical activation was conducted by ball-milling of 6.5 g of the powder in a 45 cm^3 tungsten carbide jar, with tungsten carbide balls 5 mm in diameter (the powder-to-ball ratio was 1:20), in a planetary micro mill (PULVERISETTE 7 premium line, FRITSCH). The mechanical activation was conducted for 0, 5, 10, 30, 60, 90, and 120 min, in the air. The mechanically activated samples were pressed into discs of 8 mm in diameter, under 78.45 MPa. Isothermal sintering of the samples was carried out in a chamber furnace at 1300^{o}C (2 h, in air) and used for dielectric measurements. The sintered samples were labeled as STOS0, STOS5, STOS10, STOS30, STOS60, STOS90 to STOS120, according to the corresponding time of activation.

Microstructure of $SrTiO_3$ ceramics were analyzed by a scanning electron microscope (SEM). Measurements were conducted using JSM-6390 LV JEOL (25 kV), where sample tablets were crushed and coated with gold (Au).

The X-ray diffraction patterns were obtained using a Rigaku Ultima IV diffractometer in Bragg-Brentano geometry, with Cu-K_α radiation, at room temperature, at angles 2θ of 10-90 ^{o} with a step of 0.02 ^{o} and collection time of 2s. Rietveld analysis was performed with full refinement using the GSAS II software package [42]. The obtained values of R_{wp} (weighted residual factor) varied from 6.0 % to 14.1 % and the Goodness of Fit indicator was GoF~1.

Raman spectra were taken in the spectral range of 60–1200 cm^{-1} at room temperature, with a Horiba JobinYvonLabRam ARAMIS Raman system, using the 633 nm line of a He-Ne laser. Data was collected using a count time of 5 s with five averaging cycles. The samples were measured under a microscope using a 100x objective. TO_2 Raman mode was fitted to determine the asymmetry factor *q*.

The dielectric parameters were measured at room temperature (25^{o}C) in a frequency range from 0.3 MHz to 3 GHz. Powders were pressed into a disc form (green pellets), with a diameter around 7.04 mm and thickness around 1 mm. The density of sintered samples varied from 3.9 to 4.4 gcm^{-3}, depending on the sample. The silver paste was added to the top and bottom surfaces of sintered discs to ensure good contact of the material with the electrodes [43].

3. Results and Discussion

In order to determine the structural characteristics, sintered samples were examined using X-ray diffractometry (XRD). The results showed no observable secondary phases in all $SrTiO_3$ samples sintered at 1300^{o}C for 2 h (Fig. 1). The structural parameters of the samples were refined by Rietveld's profile-fitting method and the final structural parameters of Rietveld's analysis are summarized in Tab. I.

Tab. I Microstructural parameters of $SrTiO_3$ obtained using Rietveld and SEM analysis.

Activation time (min)	**$SrTiO_3$ lattice parameter ($\dot{A}$)**	**Crystallite size (nm)**	**Microstrain (%)**	**Mean grain size (μm)**	**Mean pore size (μm)**
0	3.9045±0.0001	345±10	0.011±0.001	1.23	1.63
5	3.9049±0.0001	230±10	0.015±0.001	1.34	1.37
10	3.9054±0.0001	210±10	0.019±0.001	1.49	0.96
30	3.9048±0.0001	280±10	0.034±0.001	1.67	1.56
60	3.9044±0.0001	500±10	0.024±0.001	2.02	2.50
90	3.9056±0.0001	460±10	0.021±0.001	1.45	1.67
120	3.9060±0.0001	300±10	0.022±0.001	1.75	1.16

It is well known that mechanical activation of the starting material causes a reduction in particle size, which increases the contact surface between particles, as well as the surface free energy and Gibbs free energy [44]. This effect leadsto an increase in the reactivity of raw materials [45], enhancing the sintering process [44]. In samples activated for 5-10 min, it was noticed that the average crystallite size has lower values compared to the non-activated sample (230 and 210 nm) which is a consequence of the comminution of the starting powder particles due to mechanical activation [46]. On the other hand, in the samples activated longer than 10 min, secondary agglomeration causes the average crystallite size to increase compared to the non-activated sample. This suggests that mass transport is more intense

within hard agglomerates, where the recrystallization process begins at lower temperatures, resulting in larger crystallites (new mosaic blocks).

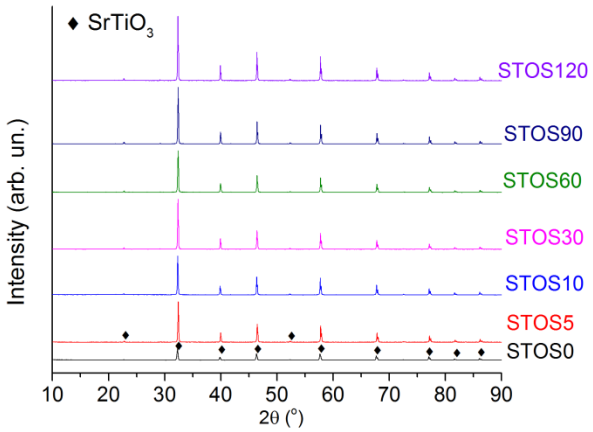

Fig. 1. XRD patterns of the $SrTiO_3$ ceramics sintered in air at 1300°C for 2 h.

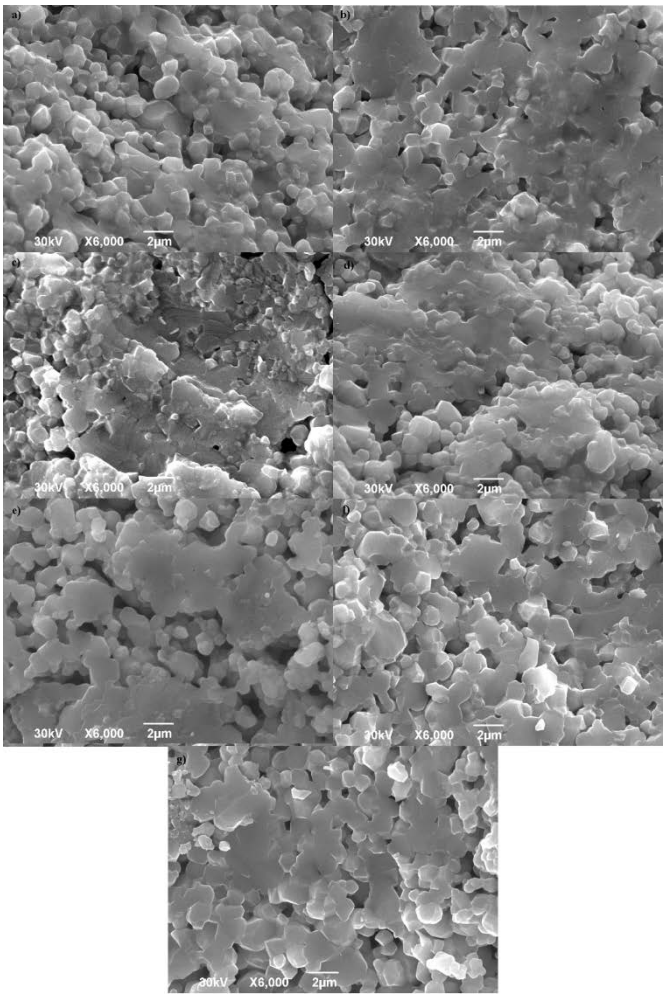

Fig. 2. SEM microstructures of $SrTiO_3$ samples sintered at 1300°C for 2 h, obtained: a) from non-activated powders and powders activated for 5, 10, 30, 60, 90, and 120 min (b-g), respectively.

The values of microstrain are relatively low: varying from 0.011 to 0.034 %, indicating low concentrations of defects due to their elimination during sintering (Tab. I). The values of the lattice parameter *a* change with the time of activation, which is a consequence of the presence of oxygen vacancies after the sintering process [47]. Samples activated for 30 and 60 min showed a decrease in lattice parameter *a*, due to dominant sintering inside agglomerates where surface defects from intra-agglomerate grains are eliminated more quickly. The highest values of lattice parameter *a* were observed for samples activated for 90 and 120 min, indicating a presence of higher concentrations of oxygen vacancies.

SEM analysis of non-activated sample showed a relatively porous microstructure where particles retained their shape (Fig. 2a). This is typical for the initial stage of sintering. Pores are irregular in shape and the mean pore size diameter is around 1.63 μm, while the mean grain size diameter is about 1.23 μm (Tab. I).

Mechanical activation leads to the amplification of transport processes, resulting in a more compact microstructure of samples STOS5 and STOS10 (Fig. 2b,c). STOS5 sample has a more uniform grain size distribution compared to the STOS10 sample. In the pre-sintered sample of STOS30, the presence of agglomerates was observed – they play an important role during material processing, which includes both their influence on powder compacting and further sintering [46]. Type of agglomerates, their size distribution, and relative density are related to the development of microstrain and the formation of microstructural defects, as well as to reinforced grain growth during sintering [44,46]. In this system, it was observed that mechanical activation produces more compact agglomerates, suggesting that it would promote grain growth (Fig. 2d, Tab. I). For activation longer than 30 minutes, enhanced sintering of the grains within the agglomerates was observed, followed by increased inter-agglomerate porosity (Fig. 2e). The non-spherical shape of pores, even in the samples activated for longer than 60 min, suggests that the sintering has not entered the final stage. In sintered STOS120 sample (Fig. 2g), a larger proportion of smaller particles was formed, with broader non-uniform distributions of particle and pore sizes (Fig. 3).

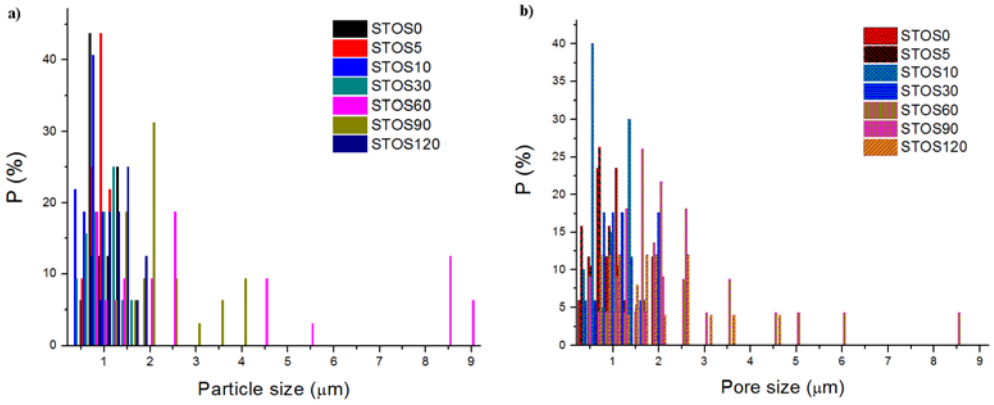

Fig. 3. a) Particle and b) pore size distribution for $SrTiO_3$ sintered samples obtained from powders non-activated and activated for 5, 10, 30, 60, 90, and 120 min.

It is known that pure strontium titanate without structural defects and microstrain has an ideal cubic perovskite structure at room temperature with Pm3m space group [48], and vibrational modes $4F_{1u}+F_{2u}$, where one of the F_{1u} vibration modes is acoustic, while F_{2u} is an inactive ("silent") mode. Since the $3F_{1u}$ IR-active modes are Raman inactive, first-order Raman scattering is not expected at room temperature for an ideal $SrTiO_3$ crystal and its Raman spectrum should correspond to the second-order scattering [49]. The presence of oxygen vacancies and other defects can break the central symmetry of $SrTiO_3$, leading to the

appearance of first-order Raman modes in bulk $SrTiO_3$, even at temperatures much higher than the regular phase transition temperature [49,50].

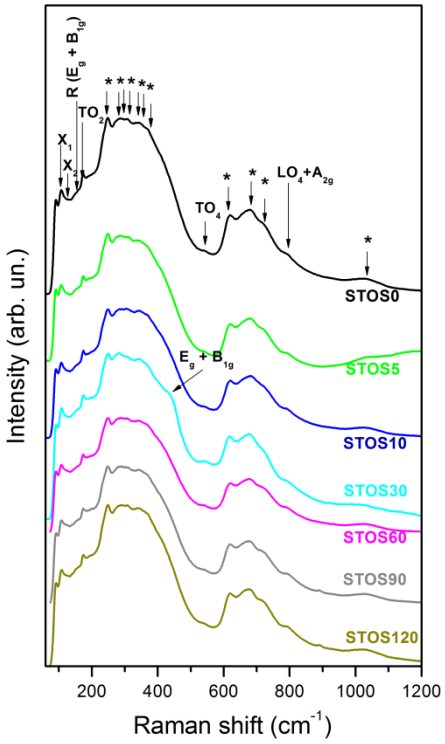

Fig. 4. Raman spectra of non-activated and activated $SrTiO_3$ samples sintered on 1300°C for 2 h.

Raman peaks of non-activated and mechanically activated samples sintered at 1300°C (2 h, in air) were investigated in the range from 60 cm^{-1} to 1200 cm^{-1} (Fig. 4). Two broad Raman effects, consisting of a large number of modes derived from second-order scattering, were observed in the Raman shift range from 220 cm^{-1} to 500 cm^{-1} and 590 cm^{-1} to 760 cm^{-1}, respectively [49]. The additional second-order mode was noticed at 1026 cm^{-1}. The first-order peaks at 174 cm^{-1}, 540 cm^{-1}, and 790 cm^{-1} were also observed and they may be assigned to TO_2 (within the doublet (LO_1+TO_2)) and TO_4 modes, as well as to doublet (LO_4+A_{2g}), respectively. These peaks can be associated with Sr-TiO_3 vibrations (174 cm^{-1}) and the Ti-O stretching vibrations (540 cm^{-1}) [51-53]. The occurrence of all these first-order Raman peaks indicates that the breaking of crystal symmetry takes place, which is consistent with previous work on $SrTiO_3$ thin-film and ceramic samples [50,53-55]. Barely noticeable R(E_g+B_{1g}) peak at 150 cm^{-1} originates from R-point at the border of Brillouin zone, while X_1 and X_2 modes at 107 cm^{-1} and 127 cm^{-1} can be attributed to the existence of polar nano or microregions induced by defects in the crystal lattice, such as oxygen vacancies [56,57].

The intensity of the Raman-modes in the range from 220 to 400 cm^{-1} slightly decreases with an increase in the activation time up to 60 min, after which an increase in its intensity occurs. The broadening of this effect with activation up to 30 min is followed by the appearance of the mode (E_g+B_{1g}) at 430 cm^{-1}, and some amplification of TO_4 mode in the STOS30 sample.

Blue shifts of TO_4 mode and TO_2 mode with an increase in activation time are negligible (up to 1 cm^{-1}) in sintered samples, with respect to the shifts which were noticed in pre-sintered mechanically activated powders [46]. However, some changes in the broadening and asymmetry of the TO_2 mode were observed. The polar TO_2 phonon shows a typical Fano

asymmetry (Fig. 5a) which is attributed to its interaction with polarization fluctuations in local polar nano or microregions, typically caused by oxygen vacancies [58-60]. The asymmetry parameter *q* is indicative of the interaction of the dielectric continuum with the polar phonon, due to polarization fluctuations in defect-induced ferroelectric nano-polar regions [60]. The value of asymmetry parameter *q* is negative, which is typical for the case of interference with the electronic continuum [49]. Some of the authors have indicated that the appearance of the TO_2 mode is usually accompanied by the appearance of remanent polarization, while the intensity of this mode is proportional to the total volume of polar micro-regions [50,61,62]. An increase in the intensity of the polar TO_2 mode also indicates an increase in the volume of local ferroelectric domains, which coexist with the dominant paraelectric phase [63].

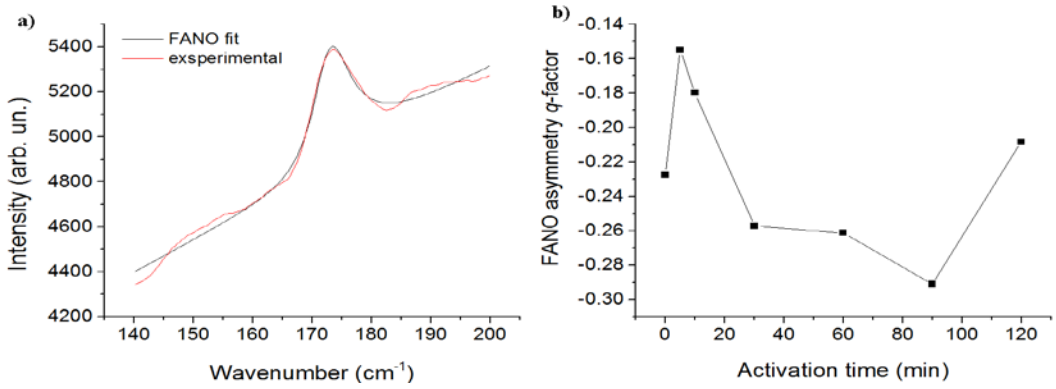

Fig. 5. FANO fit for the TO_2 peak: a) of sample activated for 5 min. and b) dependence of asymmetry factor *q* on mechanical activation time.

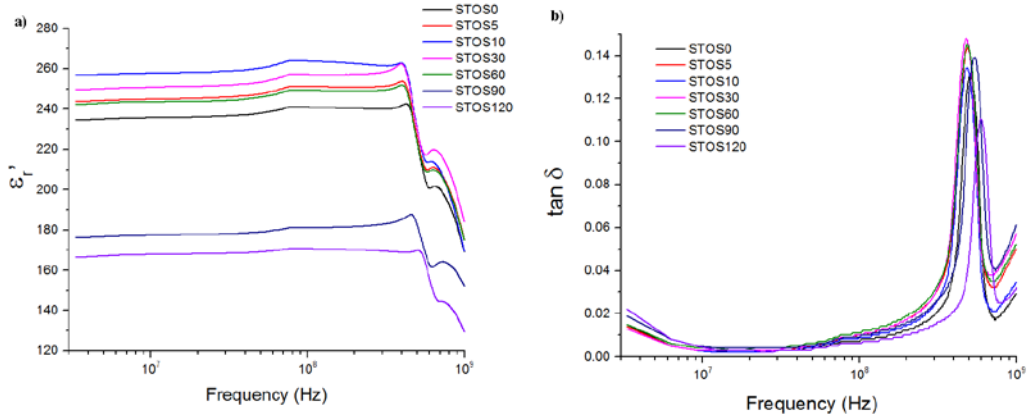

Fig. 6. a) ε_r' and b) loss tangent as a function of frequency for samples STOS0, STOS5, STOS10, STOS30, STOS60, STOS90, and STOS120, at 25°C.

Dielectric permittivity depends on grain size, sample density and presence of the polar layer at the grain boundary among other impacts [15-17]. Mechanical activation affects grain size, but also the concentration of defects and microstrains, especially in surface layers of the grain [64]. Dielectric measurements showed that mechanical activation had a significant impact on the dielectric properties of strontium-titanate samples [65]. Fig. 6a shows the relaxation type of dielectric behavior at about 0.4 GHz in all samples. In the case of $SrTiO_3$ single crystal, dielectric dispersion is expected in the terahertz region, while for ceramic samples some additional dielectric dispersion occurs in the microwave region due to

the existence of a polar layer on the grain boundary [41,66,67]. The presence of this polar layer, even in nominally pure $SrTiO_3$ ceramics, could explain the appearance of first-order Raman modes which indicate the existence of local distortion of the cubic structure. The decrease in relative dielectric permittivity due to dielectric relaxation process is accompanied by an increase in loss tangent (Fig. 6b).

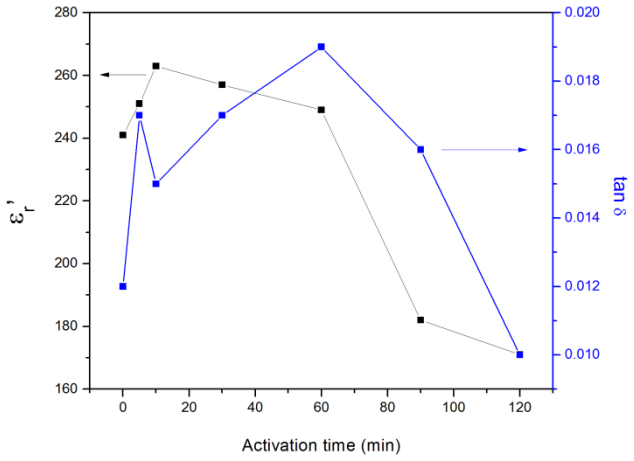

Fig. 7. Dependencies of relative permittivity and loss tangent of activation time, measured at the frequency of 200 MHz.

Fig. 7 shows dependencies of relative permittivity and loss tangent on activation time, measured at the frequency of 200 MHz for non-activated and activated samples at 25°C.

For $SrTiO_3$ ceramic, when grain size increases the value of ε_r' also increases when the diameters of the grains are up to 1.5 microns [64]. In our research it has been observed that relative dielectric permittivity changes with the time of mechanical activation: it increases up to 10 min of activation and then begins to decrease with prolonged activation, with a significant drop occurring for mechanical activation longer than 60 min. This decrease in permittivity may be caused by the secondary agglomerations in longer activated powders, which led to more difficult polarization process in sintered samples [68]. Although mean grain size is larger in STOS5 and STOS10 samples, than in the STOS0 sample, it is still less than 1.5 μm, with the presence of more uniform particle size distribution and a lower degree of porosity (Tab. I). In the case of samples activated for 30 and 60 min a further increase in the mean grain size is observed, with values greater than 1.5 μm (Tab. I). Correspondingly, the value of dielectric permittivity decreases (Fig. 7). The decrease in ε_r' was also observed in samples STOS90 and STOS120 as a result of a reduced degree of ion polarization inside the grain and/or inside the grain boundary region.

Changes in ε_r' can also be associated with the observed changes in the Raman spectra (Fig. 4). Higher values of factor q in STOS5 and STOS10 samples indicate a stronger interaction between TO_2 mode and dipole moments in the local polar regions, so a higher value of ε_r' at room temperature is expected [69,70]. Considering the detected changes in q factor, a futher decrease in ε_r' with increased time of activation up to 90 minutes was expected as well. These observations are in agreement with the literature data which indicates that the appearance of the first-order Raman modes in ceramics, as well as the values of ε_r', are significantly influenced by the grain boundary, where the concentration of localized point defects (such as oxygen vacancies) can be much larger than average. In the area of grain boundary, a layer of localized ("*frozen*") dipoles can be formed even at room temperature, which influences the Raman spectrum and the values of relative dielectric permittivity [88]. The discrepancy in the change in the values of q factor and ε_r' for the sample activated for

120 min, is a consequence of the increased influence of factors such as porosity, grain size, and density, compared to the influence of localized point defects.

4. Conclusion

Mechanical activation of $SrTiO_3$ powders leads to structural changes so that the functional properties of the ceramic materials are a direct consequence of these changes. The analysis of the morphology of the sintered samples showed that the increase in mechanical activation time results in more compact samples, as a result of the amplification of the mass transport processes and increase in grain size. Rietveld analysis indicated that the value of the crystal lattice parameter *a* in sintered $SrTiO_3$ samples is lower compared to that in powders, which is correlated with the decrease in the concentration of defects during the sintering process. The polar TO_2 phonon Raman mode showed a typical Fano asymmetry, which indicated its interaction with polarization fluctuations in polar microregions, caused by the presence of defects such as oxygen vacancies. All samples show dielectric relaxation above 0.4 GHz, which is not characteristic of bulk cubic $SrTiO_3$. The value of dielectric permittivity depends on the duration of mechanical activation: the sample activated for 10 minutes has the highest permittivity value. It can be concluded that the values of relative dielectric permittivity in the radio frequency range are stable, which is important for the fabrication of electronic components.

Acknowledgments

Funds for the realization of this work are provided by the Ministry of Education, Science and Technological Development of the Republic of Serbia, Agreement on realization and financing of scientific research work of the: Institute of Technical Sciences of SASA in 2022 (Record number: 451-03-68/2022-14/200175), University of Belgrade, Faculty of Mechanical Engineering (Record number: 451-03-68/2022-14/200105), University of Belgrade, Faculty of Agriculture (Record number: 451-03-68/2022-14/200116), and the National Science Foundation grants HRD-1345219 and DMR-1523617, and the Department of Energy/National Nuclear Security Administration NA0003979 award.

5. References

1. L. Amaral, A.M.R. Senos, P. M. Vilarinho, "Sintering kinetic studies in nonstoichiometric strontium titanate ceramics", Mater. Res. Bull 44 (2009) 263-270.
2. A. Shkabko, M. H. Aguirrea, I. Marozau, M. Doebeli, M. Mallepell, T. Lippert, A. Weidenkaff, "Characterization and properties of microwave plasma-treated SrTiO3", Mater. Chem. Phys. 115 (2009) 86-92.
3. F. M. Pontes, E.J.H. Lee, E. R. Leite, E. Longo, J. A. Varela, "High dielectric constant of $SrTiO_3$ thin films prepared by chemical process", J. Mater. Sci. 35 (2000) 4783-4787.
4. H. Zhao, Z. Fan, Q. Fu, H. Wang, Z. Hu, H. Tao, X. Zhang, Z. Ma, T. Jia, "Enhanced photocatalytic performance of $SrTiO_3$ crystals with (100), (110) and (111) orientations treated by N_2 (H_2) plasma", J. Mater. Sci. 53 (2018) 15340-15347.

5. A. Tkach, P. M. Vilarinho, A. L. Kholkin, "Dependence of dielectric properties of manganese-doped strontium titanate ceramics on sintering atmosphere", Acta Mater. 54 (2006) 5385-5391.
6. A. K. Tagantsev, V. O. Sherman, K. F. Astafiev, J. Venkatesh, N. Setter, "Ferroelectric Materials for Microwave Tunable Applications", J. Electroceram. 11 (2003) 5-66.
7. D. Zhang, T. W. Button, V. O. Sherman, A. K. Tagantsev, T. Price, D. Iddles, "Effects of glass additions on the microstructure and dielectric properties of barium strontium titanate (BST) ceramics", J. Eur. Ceram. Soc. 30 (2010) 407-412.
8. K. Xu, M. Yao, J. Chen, P. Zou, Y. Peng, F. Li, X. Yao, "Effect of crystallization on the band structure and photoelectric property of $SrTiO_3$ sol-gel derived thin film", J. Alloys Compd. 653 (2015) 7-13.
9. G. Wu, P. Li, D. Xu, B. Luo, Y. Hong, W. Shi, C. Liu, "Hydrothermal synthesis and visible-light-driven photocatalytic degradation for tetracycline of Mn-doped SrTiO3 nanocubes", Appl. Surf. Sci. 333 (2015) 39-47.
10. F. Zaza, G. Orio, E. Serra, "Quality by design approach for SrTiO3 perovskite nanomaterials synthesis", J. Mater. Sci. 51 (2016) 9649-9668.
11. L. F. da Silva, L. J. Q. Maia, M. I. B. Bernardi, J. A. Andrés, V. R. Mastelaro, "An improved method for preparation of $SrTiO_3$ nanoparticles", Mater. Chem. Phys. 125 (2011) 168-173.
12. K. Kavitha, T. Vijayaraghavan, N. Gouthami, V. Udhayabanu, Anuradha M. Ashok, "Solid-state synthesis and electrical conductivity properties of Ba3SrTa2O9 complex perovskite", Mater. Charact. 133 (2017) 17-24.
13. X. Liu, H. Bai, "Liquid-solid reaction synthesis of SrTiO3 submicron-sized particles", Mater. Chem. Phys. 127 (2011) 21-23.
14. S. Neogi, U. Chowdhury, A.-K. Chakraborty, J. Ghosh, "Effect of mechanical milling on the structural and dielectric properties of BaTiO3 powders", IET Micro & Nano Letters 10 (2015) 109-114.
15. L. Wu, M. C. Chure, K. K. Wu, W. C. Chang, M. J. Yang, W. K. Liu, M. J. Wu, "Dielectric properties of barium titanate ceramics with diffrent materials powder size", Ceram. Int. 35 (2009) 957-960.
16. S. Neogi, U. Chowdhury, A. K. Chakraborty, J. Ghosh, "Effect of mechanical milling on the structural and dielectrical properties of BaTiO3 powders", Micro Nano Lett. 10 (2015) 109-114.
17. R. L. Coble, “Effects of particle-size distribution in initial-stage sintering.” J. Am. Cerami. Soc. 56 (1973) 461-466.
18. C. R. K. Monah, P. K. Bajpai, "Effect of sintering optimization on the electrical properties of bulk BaxSr1-xTiO3 ceramics", Physica. B. (2007) 2713-2188.
19. A. Friederich, X. Zhou, M. Sazegar, J. Haubelt, R. Jakoby, M.J. Hoffmann, J.R. Binder, "The influence of processing on the microstructure and the microwave properties of Co-F-codoped barium strontium titanate thick-films", J. Eur. Ceram. Soc. 32 (2012) 875-882.
20. C. Ang, Z. Yu, L. E. Cross, "Oxygen-vacancy-related low-frequency dielectric relaxation and electrical conduction in Bi:$SrTiO_3$", Phys. Rev. 62 (2000) 228-236.

21. Z. Yu, C. Ang, R. Guo, A.S. Bhalla, L.E. Cross, "Dielectric loss modes of $SrTiO_3$ thin films deposited on different substrates", Appl. Phys. Lett. 80 (2002) 1034-1036.
22. W. Wang, C. Jiang, M. Shen, L. Fang, F. Zheng, X. Wu, J. Shen, "Effect of oxygen vacancies on the red emission of $SrTiO_3$: Pr^{3+} phosphor films", Appl. Phys. Lett. 94 (2009) 081904.
23. Darko Kosanović, Jelena Živojinović, Jelena Vujančević, Adriana Peleš, Vladimir A. Blagojević, "Point Defects and their Effect on Dielectric Permittivity in Strontium Titanate Ceramics", Sci. Sinter. 53 (2021) 0285-299.
24. A. Tkach, L. Amaral, P. M. Vilarinho, A. M. R. Senos, "Oxygen vacancies as a link between the grain growth and grain boundary conductivity anomalies in titanium-rich strontium titanate", J. Eur. Ceram. Soc. 38 (2018) 2547-2552.
25. A. Tkach, P.M. Vilarinho, A.M.R. Senos, A.L. Kholkin, "Effects of nonstoichiometry on the microstructure and dielectric properties of strontium titanate ceramics", J. Eur. Ceram. Soc. 25 (2005) 2769-2772.
26. H.P.R. Frederikse, W. R. Thurber, W. R. Hosler, "Electronic Transport in Strontium Titanate", Phys. Rev. 134 (1964) A442-A445.
27. V. V. Lemanov, A. V. Sotnikov, E. P. Smirnova, M. Weihnacht, "Giant dielectric relaxation in SrTiO3-Sr/Mg1/3Nb2/3O3 and SrTiO3-SrSc1/2Ta1/2O3 solid solutions", Phys. Solid State 44 (2002) 2039-2049.
28. A. Tkach, P.M. Vilarinho, A.L. Kholkin, "Structural and Dielectric Properties of Mn-Doped Strontium Titanate Ceramics", Ferroelectrics 304 (2004) 87-90.
29. A. Tkach, P.M. Vilarinho, A.L. Kholkin, "Effect of Mg doping on the structural and dielectric properties of strontium titanate ceramics", Appl. Phys. A 79 (2004) 2013-2020.
30. M. E. Guzhva, V. V. Lemanov, P. A. Markovin, "Dielectric studies of phase transitions in the ferroelectric $CdTiO_3$ and the $Sr_{1-x}Cd_xTiO_3$ solid solutions", Phys. Solid State 43 (2001) 2146-2153.
31. A. Tkach, P.M. Vilarinho, A.L. Kholkin, "Polar behavior in Mn-doped $SrTiO_3$ ceramics", Appl. Phys. Lett. 86 (2005) 172902.
32. F. Narita, T. Kobayashi, Y. Shindo, "Evaluation of dielectric and piezoelectric behavior of unpoled and poled barium titanate polycrystals with oxygen vacancies using phase field method", Int. J. Smart Nano Mater. 7 (2016) 265-275.
33. Y. K. Choi, T. Hoshina, H. Takeda, T. Tsurumi, "Effect of oxygen vacancy and Oxygen Vacancy Migration on Dielectric Response of $BaTiO_3$-Based Ceramics", Jpn. J. Appl. Phys. 50 (2011) 031504.
34. T. Teranishi, R. Kanemoto, H. Hayashi, A. Kishimoto, "Effect of the (Ba+Sr)/Ti ratio on the microwave-tunable properties of $Ba_{0.6}Sr_{0.4}TiO_3$ ceramics", J. Am. Ceram. Soc. 100 (2016) 1-7.
35. M. Sakurai, K. Kanehara, H. Takeda, T. Tsurumi, T. Hoshina, "Wideband dielectric spectroscopy of $(Sr_{0.7}Bi_{0.2})TiO_3$ ceramics and its microscopic mechanism of polarization", J. Ceram. Soc. Jpn. 124 (2016) 664-667.
36. H. Chazono, H. Kishi, "dc-Electrical Degradation of the BT-Based Material for Multilayer Ceramic Capacitor with Ni internal Electrode: Impedance Analysis and Microstructure", Jpn. J. Appl. Phys. 40 (2001) 5624-5629.

37. D.F.K. Hennings, H. Schreinemacher, "Ca-acceptors in dielectric ceramics sintered in reductive atmospheres", J. Eur. Ceram. Soc. 15 (1995) 795-800.
38. K. Kanehara, T. Hoshina, H. Takeda, T. Tsurumi, "Measurement of ionic polarization of $SrTiO_3$ single crystal by far-infrared spectroscopic ellipsometry", Appl. Phys. Lett. 105 (2014) 042901.
39. T. Tsurumi, T. Teranishi, S. Wada, H. Kakemoto, O. Fukunaga, M. Nakada, J. Akedo, "Ultra Wide Range Dielectric Spectroscopy of Strontium Titanate-Strontium Zirconate Solid Solution", J. Ceramic. Soc. Jpn. 114 (2006) 774-781.
40. J. Petzelt, T. Ostapchuk, A. Pashkin, I. Rychetsky, "FIR and near-millimetre dielectric response of $SrTiO_3$, $BaTiO_3$ and BST films and ceramics", J. Eur. Ceram. Soc. 23 (2003) 2627-2632.
41. T. Hoshina, R. Sase, J. Nishiyama, H. Takeda, T. Tsurumi, "Effect of oxygen vacancies on intrinsic dielectric permittivity of strontium titanate ceramics", J. Ceram. Soc. Jpn. 126 (2018) 263-268.
42. B. H. Toby, R. B. Von Dreele, "GSAS-II: the genesis of a modern open-source all-purpose crystallography software package", Journal of Appl. Crystallogr., 46 (2013) 544-549.
43. A. Đorđević, J. Dinkić, M. Stevanović, D. Olćan, S. Filipović, N. Obradović, "Measurement of Permittivity of Solid and Liquid Dielectrics in Coaxial Chambers", Microwave Review, 22 (2016) 3-9.
44. N. Behmanesh, S. Heshmati-Manesh, A. Ataie, "Role of mechanical activation of precursors in solid state processing of nano-structured mullite phase", J. Alloys Compd. 450 (2008) 421-425.
45. Lj. Andrić, Z. Aćimović Pavlović, N. Pavlović, V. Milošević, S. Milicević, "Mechanical activation of talc in high-energy speed rotary mechanoactivator", Ceram. Int. 38 (2012) 2913-2920.
46. J. Živojinović, V. P. Pavlović, D. Kosanović, S. Marković, J. Krstić,V. A. Blagojević, V. B. Pavlović, "The Influence of Mechanical Activation on Structural Evolution of Nanocrystalline $SrTiO_3$ Powders", J. Alloys Compd. 695 (2017) 863-870.
47. R. Sase, T. Hoshina, H. Takeda, T. Tsurumi, "Effect of atomic vacancies on ionic polarization of nonstoichiometric strontium titanate ceramics", Jpn. J. Appl. Phys. 56 (2017) 10PB11.
48. A. R. Benrekia, N. Benkhettou, A. Nassour, M. Driz, M. Sahnoun, S. Lebegue, "Structural, electronic and optical properties of cubic $SrTiO_3$ and KTaO3: Ab initio and GW calculations", Physica B, 407 (2012) 2632-2636.
49. S. Banerjee, D. I. Kim, R. D. Robinson, S. S. Wong, I. Herman, "Observation of Fano Asymmetry in Raman Spectra of $SrTiO_3$ and Related Perovskite Nanocubes", Appl. Phys. Lett. 89 (2006) 223130.
50. A. Tkach, P. M. Vilarinho, A. L. Kholkin, A. Pashkin, S. Veljko, J. Petzelt, "Broad-band dielectric spectroscopy analysis of relaxational dynamics in Mn-doped $SrTiO_3$ ceramics", Phys. Rev. B, 73 (2006) 104113.
51. M. L. Moreira, V. M. Longo, W. Avansi Jr., M. M. Ferrer, J. Andreś, V. R. Mastelar, J. A. Varela, É. Longo, "Quantum Mechanics Insight into the Microwave Nucleation of $SrTiO_3$ Nanospheres", J. Phys. Chem. C, 116 (2012) 24792-24808.

52. Y. I. Yuzyuk, "Raman scattering spectra of ceramics, films, and superlattices of ferroelectric perovskites: A review", Phys. Solid State, 54 (2012) 1026-1059.
53. T. Ostapchuk, J. Petzelt, V. Zelezny, A. Pashkin, J. Pokorny, I. Drbohlav, R. Kuzel, D. Rafaja, B.P. Gorshunov, M. Dressel, Ch. Ohly, S. Hoffmann-Eifert, R. Waser, "Origin of soft-mode stiffening and reduced dielectric response in SrTiO3 thin films", Phys. Rev. B, 66 (2002) 235406.
54. M. Misra, K. Kotani, I. Kawayama, H. Murakami, M. Tonouchi, "Observation of TO1 soft mode in $SrTiO_3$ films by terahertz time-domain spectroscopy", Appl. Phys. Lett. 87 (2005) 182909.
55. J. Petzelt, T. Ostapchuk, I. Gregora, I. Rychetský, S. Hoffmann-Eifert, A. V. Pronin, Y. Yuzyuk, B. P. Gorshunov, S. Kamba, V. Bovtun, J. Pokorný, M. Savinov, V. Porokhonskyy, D. Rafaja, P. Vaněk, A. Almeida, M. R. Chaves, A. A. Volkov, M. Dressel, R. Waser, "Dielectric, infrared and Raman response of undoped $SrTiO_3$ ceramics: Evidence of polar grain boundaries", Phys. Rev. B 64(2001) 184111.
56. P. Ranson, R. Ouillon, J. P. Pinan-Lucarre, Ph. Pruzan, S. K. Mishra, R. Ranjan, D. Pandey, "The Various Phases of the System $Sr_{1-x}Ca_xTiO_3$: A Raman Scattering Study", J. Raman Spectrosc. 36(2005) 898-911.
57. D. A. Tenne, I. E. Gonenli, A. Soukiassian, D. G. Schlom, S. M. Nakhmanson, K. M. Rabe, X.X. Xi, "Raman study of oxygen reduced and re-oxidized strontium titanate", Phys. Rev. B, 76 (2007) 024303.
58. S. Gupta, R. S. Katiyara, "Temperature-dependent structural characterization of sol-gel deposited strontium titanate ($SrTiO_3$) thin films using Raman spectroscopy", J. Raman Spectrosc. 33 (2002) 885-891.
59. Y. L. Du, G. Chen, M. S. Zhang, S. Z. Yang, "Phonon Characteristics of Polycrystalline Cubic $SrTiO_3$ Thin Films", Chin. Phys. Lett. 20 (2003) 1561-1564.
60. A. A. Sirenko, I. A. Akimov, J. R. Fox, A. M. Clark, H. C. Li, W. Si, X. X. Xi, "Observation of the First-Order Raman Scattering in the $SrTiO_3$ Thin Films", Phys. Rev. Lett. 82(1999) 4500-4503.
61. Y. L. Du, G. Chen, M. S. Zhang, "Investigation of structural phase transition in polycrystalline $SrTiO_3$ thin films by Raman spectroscopy", Solid State Commun. 130 (2004) 577-580.
62. X. W. Wu, D. J. Wu, X. J. Liu, "Negative pressure effects in $SrTiO_3$ nanoparticles investigated by Raman spectroscopy", Solid State Commun. 145 (2008) 255-258.
63. A. B. Shi, W.Z. Shen, "Phase transition temperature of $SrTiO_3$ ultrathin films: An annealing study by ultraviolet Raman spectroscopy", Appl. Phys. Lett. 91 (2007) 112910.
64. J. Petzelt, T. Ostapchuk, I. Gregora, D. Nuzhnyy, I. Rychetsky, K. Maca, Z. Shen, "Grain Boundary and Size Effect on bthe Dielectric, Infrared and Raman Response of $SrTiO_3$ Nanograin Ceramics", Ferroelectrics, 363 (2008) 227-244.
65. T. Hoshina, R. Sase, J. Nishiyama, H. Takeda, T. Tsurumi, "Effect of oxygen vacancies on intrinsic dielectric permittivity of strontium titanate ceramics", J. Ceram. Soc. Jpn. 126 (2018) 263-268.
66. R. Sase, T. Hoshina, H. Takeda, T. Tsurumi, "Effect of atomic vacancies on ionic polarization of nonstoichiometric strontium titanate ceramics", Jap. J. Appl. Phys. 56 (2017) 10PB11.

67. J. Petzelt, T. Ostapchuk, I. Gregora, I. Rychetsky, S. Hoffmann-Eifert, A.V. Pronin, Y. Yuzyuk, B.P. Gorshunov, S. Kamba, V. Bovtun, J. Pokorny, M. Savinov, V. Porokhonskyy, D. Rafaja, P. Vanek, A. Almeida, M. R. Chaves, A. A. Volkov, M. Dressel, R. Waser, "Dielectric, infrared and Raman response of undoped $SrTiO_3$ ceramics: Evidence of polar grain boundaries", Phys. Rev. B, 64 (2001) 184111.
68. L. C. Yan, J. Hassan, M. Hashim, W. S. Yin, T. F. Khoon,W. Y. Jeng, "Effect of Sintering Temperatures on the Microstructure and Dielectric Properties of $SrTiO_3$", World Appl. Sci. J. 14 (2011) 1091-1094.
69. A. A. Sirenko, I. A. Akimov, J. R. Fox, A. M. Clark, H. C. Li, W. Si, X. X. Xi, "Observation of the First-Order Raman Scattering in the $SrTiO_3$ Thin Films", Phys. Rev. Lett. 82 (1999) 4500-4503.
70. S. Gupta, R. S. Katiyara, "Temperature-dependent structural characterization of sol-gel deposited strontium titanate ($SrTiO_3$) thin films using Raman spectroscopy", J. Raman Spectrosc. 33 (2002) 885-891.

Сажетак: *У овом истраживању проучаван је развој микроструктуре и диелектрична својства $SrTiO_3$ керамике при чему је механичка активација $SrTiO_3$ прахова коришћена како би се модификовала функционална својства керамичког материјала. СЕМ анализа микроструктуре $SrTiO_3$ керамике је показала да увећање времена механичке активације води ка добијању мање порозних узорака. Раман спектроскопија је индиковала промене у ширини и асиметрији TO_2 моде са променом времена механичке активације. TO_2 мода је Фано асиметричног облика услед интеракције са поларизационим флуктуацијама у поларним микрорегионима који су последица присуства кисеоникових ваканција насталих услед активације. Максимална вредност диелектричне пермитивности је примећена код времена механичке активације од 10 мин. Такође, узорак активиран 10 мин има најмањи тангенс диелектричних губитака, у односу на друге механички активиране узорке, и самим тим поседује најбоље диелектричне перформансе у односу на друге узорке.*

Кључне речи: *рендгено-структурна анализа, СЕМ, Раман, диелектрична пермитивност, $SrTiO_3$ керамика.*